



The expression landscape of FOXP3 and its prognostic value in breast cancer

Jingping Li^{1,2#}, Xiangmei Zhang^{2,3#}, Beichen Liu^{2,4}, Chao Shi^{1,2}, Xindi Ma^{1,2}, Shuguang Ren^{2,5}, Xiaohan Zhao^{2,6}, Yunjiang Liu^{1,2}

¹Breast Center, The Fourth Hospital of Hebei Medical University, Shijiazhuang, China; ²Hebei Provincial Key Laboratory of Tumor Microenvironment and Drug Resistance, Shijiazhuang, China; ³Research Center, The Fourth Hospital of Hebei Medical University, Shijiazhuang, China; ⁴Haematology Center, The Fourth Hospital of Hebei Medical University, Shijiazhuang, China; ⁵Animal Center, The Fourth Hospital of Hebei Medical University, Shijiazhuang, China; ⁶Department of Radiotherapy, The Fourth Hospital of Hebei Medical University, Shijiazhuang, China

Contributions: (I) Conception and design: J Li, Y Liu; (II) Administrative support: B Liu, X Zhang; (III) Provision of study materials or patients: J Li, Y Liu; (IV) Collection and assembly of data: J Li, C Shi, X Ma; (V) Data analysis and interpretation: J Li, S Ren, X Zhao; (VI) Manuscript writing: All authors; (VII) Final approval of manuscript: All authors.

[#]These authors contributed equally to this work.

Correspondence to: Yunjiang Liu, MD, PhD. Breast Center, The Fourth Hospital of Hebei Medical University, 12 Jiankang Road, Shijiazhuang 050011, China. Email: lyj818326@outlook.com.

Background: Forkhead Box Protein 3 (FOXP3), as an essential marker of regulatory T cell (Treg) development, is reportedly overexpressed in invasive breast carcinoma (BRCA) and could be a potential prognostic factor for BRCA. However, the biological function of FOXP3 in BRCA is still unclear. In this study, we comprehensively explored the expression landscape of FOXP3 and its prognostic value in BRCA.

Methods: FOXP3 transcriptomic expression data were mainly obtained from The Cancer Genome Atlas (TCGA). The Kaplan-Meier plotter and receiver operating characteristic (ROC) curve were used to assess the prognostic and diagnostic value of FOXP3 in BRCA. UALCAN, cBio-Portal, and MethSurv were used to evaluate the genomic variation of FOXP3. Gene set enrichment analysis (GSEA) was performed to explore the FOXP3 pathways involved in BRCA. Moreover, we detected the expression of FOXP3 in 123 BRCA specimens and 5 BRCA cell lines to verify the biological value of FOXP3 in BRCA. The Kaplan-Meier method was adopted for the overall survival (OS) analysis, and a Cox proportional hazards model was used to estimate the hazard ratio (HR) for OS.

Results: FOXP3 was more highly expressed in BRCA than in normal tissues (2.808 ± 1.020 vs. 1.409 ± 0.656 , $P < 0.001$), and overexpressed FOXP3 was associated with a better prognosis. The ROC curve demonstrated a significant diagnostic value of FOXP3 in BRCA (area under the ROC curve, AUC: 0.877). Genomic analysis revealed that promoter hypomethylation of FOXP3 may be the underlying mechanism of FOXP3's upregulation in BRCA. GSEA found that FOXP3 coexpressed genes were mainly involved in the Toll-like receptor pathway, JAK/STAT pathway, cell cycle, and apoptosis. Moreover, high FOXP3 expression was an independent protective factor for OS in our 123 BRCA tissues (HR: 0.367; $P = 0.036$). *In vitro*, we found that FOXP3 knockdown with siRNA promoted migration and invasion in MCF-7 cells.

Conclusions: This study demonstrated that FOXP3 shows prognostic and diagnostic value for BRCA. We provided evidence that promoter hypomethylation and a high expression of FOXP3 were both related to a favorable prognosis in BRCA, which maybe associated with the Toll-like receptor pathway, JAK/STAT pathway, cell cycle, and apoptosis.

Keywords: Forkhead Box Protein 3 (FOXP3); breast carcinoma (BRCA); The Cancer Genome Atlas (TCGA); prognosis

Submitted May 30, 2022. Accepted for publication Jun 24, 2022.

doi: 10.21037/atm-22-3080

View this article at: <https://dx.doi.org/10.21037/atm-22-3080>

Introduction

Breast cancer (BC) is the most common malignancy and the leading cause of cancer-related deaths in women (1,2). According to the latest cancer statistics, BC has now exceeded lung cancer as the world's leading cancer, with 2,261,419 new cases worldwide in 2020 (1). Although the overall mortality of BC has been decreasing—attributed to early detection and effective systemic therapy over the past decades—it is still the leading cause of cancer deaths for women (3). BC is recognized as a highly heterogeneous disease, and its molecular classifications stratify tumors into informative subtypes and provide key prognostic signatures. At present, it is well defined that estrogen receptor (ER), progesterone receptor (PR), and human epidermal growth factor receptor 2 (HER2) could be regarded as prognostic factors in BC. Consequently, BC is currently classified as either hormone receptor-positive (HR+) luminal subtype (approximately 70%), HER2+ subtype (15–20%), or triple-negative breast cancer (TNBC) (about 15%) (4). However, current clinical treatments are still not curative due to the substantial heterogeneity of the disease and intrinsic/acquired drug resistance. Despite advances in the predictive biomarkers and molecular characterization of BC, effective personalized treatment remains elusive (5). Thus, there is an urgent need to identify more effective targets and understand the signaling pathways driving BC progression, relapse, and treatment resistance.

Forkhead Box Protein 3 (FOXP3), which is located on the short arm of the X chromosome at Xp.11.23, is the key transcription factor and well-known hallmark of immunosuppressive CD4⁺CD25⁺ regulatory T cells (Treg) (6,7). One study provided evidence that multiple types of human carcinoma cells also express FOXP3, which may play an important role in tumor pathogenesis and development (8). But the prognostic value of FOXP3 in cancer appears to be divergent. As a transcription factor, FOXP3 may play a regulatory role by directly binding to specific tumor-related genes in BC (9). This ability of transcriptional regulation may well be the potential superiority of FOXP3 in relative to prior biomarkers of BC. It has been reported that FOXP3 can inhibit the transcription of the proto-oncogene HER2 (10) and the expression of runt-related transcription factor 1 (RUNX1) (11), vascular endothelial growth factor (VEGF) (12), and metastasis-associated 1 (MTA1) (13) to perform its anticancer function in BC. However, the biological function and

molecular mechanism of FOXP3 in BC have not been fully illustrated. The multiple mechanisms underlying the tumor-inhibitory capability of FOXP3 need more comprehensive and specific research.

In this study, we explored the expression landscape of FOXP3 and provided further insights into the involved mechanisms in BRCA. It revealed that FOXP3 may be a potential novel biomarker for the diagnosis and prognosis of BRCA and a potential candidate target for BRCA treatment, expecting to provide a new direction for clinical management in BRCA. We present the following article in accordance with the REMARK reporting checklist (available at <https://atm.amegroups.com/article/view/10.21037/atm-22-3080/rc>).

Methods

This study comprehensively explored the prognostic and diagnostic value of FOXP3 expression and its genomic variation in invasive breast carcinoma (BRCA), mainly using data from The Cancer Genome Atlas (TCGA) database. Moreover, we performed a gene set enrichment analysis (GSEA) analysis to explore FOXP3 coexpression genes and the involved signaling pathways in BRCA. Additionally, we detected FOXP3 expression in our BC specimens and cell lines to validate the biological function of FOXP3 in BRCA. The Kaplan-Meier method and the unstratified log-rank test were used for the survival analysis. Meanwhile, a Cox proportional hazards model was applied to ascertain the independent prognostic role of FOXP3.

Data mining

This study included the RNA sequence transcriptomic data from 1,109 patients with BRCA and 113 normal tissues downloaded from TCGA database (<https://cancergenome.nih.gov>). The RNA-seq data and the corresponding patient clinical information (Workflow Type: HTSeq-TPM) were acquired using the Data Transfer tool. To investigate the biological function of FOXP3, patients with BRCA were divided into high- and low-FOXP3 expression groups based on the median expression level. We used statistical packages R software (version 3.6.3) to download the FOXP3 mRNA expression and clinical data in the GES2034 dataset from the Gene Expression Omnibus (GEO) databases and used PrognoScan (<http://dna00.bio.kyutech.ac.jp/PrognoScan/index.html>) as an external validation of the survival analyses.

FOXP3 expression and prognostic analysis in BRCA

The Kaplan–Meier plotter (kmplot.com/analysis) is a meta-analysis-based database for the discovery and validation of survival biomarkers in cancers, including approximately 54k genes (mRNA, miRNA, and protein) in 21 cancer types (14). In our research, we evaluated the biological relationship between FOXP3 expression and survival outcomes in BRCA. Similarly, the cohorts were divided into two groups according to the median expression of FOXP3 and were compared in terms of relapse-free survival (RFS), overall survival (OS), and distant metastasis-free survival (DMFS). The hazard ratios (HRs) were computed with 95% CIs and log-rank P values.

Diagnostic value of FOXP3 in BRCA

The diagnostic role of FOXP3 in BRCA was assessed by a receiver operating characteristic (ROC) curve analysis based on TCGA data, which were downloaded from the UCSC Xena database (xena.ucsc.edu/). Our study selected the TCGA BRCA cohort and extracted the gene expression RNAseq (HTSeq-FPKM) data of FOXP3 (ENSG00000049768) (n=1,222). Then, we generated the ROC curve for FOXP3 expression in BRCA and calculated the area under the ROC curve (AUC) to evaluate the prognostic value of FOXP3.

FOXP3 expression and methylation pattern in BRCA

UALCAN (<http://ualcan.path.uab.edu/index.html>) is a comprehensive database to perform in-depth analyses of TCGA gene expression data (15). FOXP3 expression data were obtained using the “TCGA Analysis” module of UALCAN and the “BRCA” dataset. Herein, we generated the FOXP3 expression profile and its promoter methylation status based on the different clinical characteristics of BRCA. MethSurv (<https://biit.cs.ut.ee/methsurv/>) is a web portal for survival analysis based on different CpG methylation patterns (16). In our study, we used the MethSurv data to analyze the FOXP3 methylation profile and its influence on the prognosis of BRCA patients. The significance level was 0.05.

Genomic analysis of FOXP3

The cBio Cancer Genomics Portal (cBio-Portal) (www.cbioportal.org/) is an open web that contains more than

5,000 tumor samples from 20 cancer studies currently, which is accessible for interactive exploration of multidimensional cancer genomics data (17). In this study, we mainly used the cBioPortal database to evaluate the somatic mutation and copy number variation (CNV) profile of FOXP3 in BRCA.

Coexpression gene of FOXP3 and pathway enrichment analysis in BRCA

Expression profiles (HTSeq-TPM) were compared between the high and low FOXP3 mRNA expression groups to identify the differentially expressed genes (DEGs) using the unpaired Student’s *t*-test, within the Limma package software (18). A $|\log_2\text{Fold Change}| > 2$ and adjusted $P < 0.05$ were considered the threshold for the DEGs. The GSEA analysis in the R package (v3.6.3) (19) was carried out to explore the potential biological function of FOXP3 expression on the prognosis of BRCA. The functional pathway with an adjusted $P < 0.05$, a false discovery rate (FDR) < 0.25 , and a normalized enrichment score (NES) > 1 was considered to be significantly enriched.

BRCA patients and specimens

This study included 123 females with BRCA and 20 cases of benign breast fibroadenoma who underwent primary surgery without any neoadjuvant therapy at the Breast Center of the Fourth Hospital of Hebei Medical University from January 2009 to April 2012. After surgery, most patients received standardized adjuvant chemotherapy or hormone therapy. However, none of the patients received HER2-targeted treatment due to the drug unavailability in China at that time. All patients were followed up after surgery until the date of death or February 2022. OS was calculated from the time of diagnosis to the time of death from any cause or the final follow-up date. The baseline characteristics of the 123 patients in this study are shown in *Table 1*. The study was conducted in accordance with the Declaration of Helsinki (as revised in 2013). The study was approved by institutional ethics committee of the Fourth Hospital of Hebei Medical University (No. 2018MEC116). Informed consent was taken from all the patients.

Immunohistochemistry and evaluation

FOXP3 expression was analyzed immunohistochemically on paraffin-embedded tumor sections (123 BRCA tissues and

Table 1 FOXP3 expression according to the clinicopathological parameters of our BRCA patients

Characteristic	N=123	Nuclear FOXP3 expression, n (%)		P
		Low (n=64)	High (n=59)	
Age, years				0.484
<50	68	35 (51.5)	33 (48.5)	
≥50	55	29 (52.7)	26 (47.3)	
Tumor size, cm				0.902
≤2.0	66	34 (51.5)	32 (48.5)	
>2.0	57	30 (52.6)	27 (47.4)	
Lymph nodes				0.308
Negative	65	31 (47.7)	34 (52.3)	
Positive	58	33 (56.9)	25 (43.1)	
TNM stage				0.106
I	37	14 (37.8)	23 (62.2)	
II	67	38 (56.7)	29 (43.3)	
III	19	12 (63.2)	7 (36.8)	
Histologic grade				0.766
1	26	13 (50.0)	13 (50.0)	
2	75	38 (50.7)	37 (49.3)	
3	22	13 (59.1)	9 (40.9)	
Vessel tumor embolus				0.024
Negative	86	39 (45.3)	47 (54.7)	
Positive	37	25 (67.6)	12 (32.4)	
Ki67				0.041
Low (≤30%)	39	15 (38.5)	24 (61.5)	
High (>30%)	84	49 (58.3)	35 (41.7)	
ER/PR				0.092
Negative	57	25 (43.9)	32 (56.1)	
Positive	66	39 (59.1)	27 (40.9)	
HER2				0.596
Negative	78	42 (53.8)	36 (46.2)	
Positive	45	22 (48.9)	23 (51.1)	
Subtype				0.207
Luminal	66	39 (59.1)	27 (40.9)	
HER2	32	13 (40.6)	19 (59.4)	
TNBC	25	12 (48.0)	13 (52.0)	

BRCA, breast carcinoma; ER, estrogen receptor; PR, progesterone receptor; HER2, human epidermal growth factor receptor 2; TNBC, triple-negative breast cancer.

20 breast fibroadenoma tissues) using a mouse antihuman FOXP3 monoclonal antibody (clone ab20034, 1:50 dilution; Abcam, Cambridge, UK). The antigen retrieval was carried out by heating slides for 15 minutes at 95 °C in citrate buffer (pH 6.0). A blocking reagent was added after quenching the endogenous peroxidase activity in 0.3% hydrogen peroxide. Specimens were incubated with the FOXP3 antibody at 4 °C overnight. Then, immunodetection was performed with biotinylated anti-mouse immunoglobulin for 30 minutes at room temperature, followed by 3,3'-diaminobenzidine chromogenic as a substrate to visualize the slides and Harris hematoxylin for counterstaining. Positive and negative staining controls were carried out with paraffin tonsil sections using the same antibody above and an appropriate isotype-matched negative control (NC) antibody (mouse IgG1, ZSGB-BIO, China). The staining was interpreted by two of the authors, both blinded to the clinicopathological data. Discrepancies were reviewed jointly, and a consensus was reached.

FOXP3 expression in cell lines and siRNA transfection

The Human Protein Atlas (HPA) (www.proteinatlas.org) is an interactive resource offering a unique opportunity to explore and map all human protein-coding genes in cells, tissues, and organs by integrating data from TCGA, GTEx consortium, and recount2 (20). We used the “Cell Line” module to investigate the FOXP3 expression profile in human cancer cell lines.

In addition, we purchased five BRCA cell lines (MCF-7, MDA-MB-231, MDA-MB-453, BT-474, and SK-BR-3) from the American Type Culture Collection (ATCC) bank and cultured these cells in 10% FBS + RPMI1640 in our laboratory. The FOXP3 siRNA and NC were designed and purchased from GenePharma (Shanghai, China). The most effective targeted sequences are followed siFOXP3: 5'-CUG CCU CAG UAC ACU CAA ATT-3'. The siRNA transfection was performed by using a FuGENE HD transfection reagent (Promega, USA) according to the manufacturer's protocol. After transfection and culture for 48 hours, the cells were collected.

Quantitative real-time PCR and western blot

The total RNA in cells was extracted with a trizol reagent (Invitrogen, USA), and the relative mRNA expression was normalized to the GAPDH (Forward: 5'-

CAAGGCTGAGAACGGGAA-3'; Reverse: 5'-GCATC GCCCACTTGATTTT-3'). The FOXP3 primer was purchased from ThermoFisher SCIENTIFIC (Shanghai, China) (Forward: 5'-GTGGCCCCGGATGAGAAG-3'; Reverse: 5'-GGAGCCCTTGTCCGATGATG-3'). Quantitative real-time PCR was performed as previously described. A western blot assay was used to validate the downregulation of FOXP3 protein expression in the si-FOXP3 group, with β -actin used as the loading control. A FOXP3 primary antibody (clone ab20034, Abcam, Cambridge, UK) with a working concentration of 1:1,000 was used in the western blot.

Migration and invasion assays

A wound-healing assay in a 6-well plate was conducted to detect the influence of FOXP3 expression on the migration ability of MCF-7 cells. When the cells grew to 70% density, the fused monolayer cells were scratched with a 10 μ L sterile pipette and washed twice with PBS to remove cell debris. Then, a serum-free medium was added to the wells. After incubation for 24 hours at 37 °C, scratch images were taken using a microscope. For the invasion experiment using a transwell chamber, 50 μ L of Matrigel matrix (1:8) was first placed in the upper chamber, and the chamber was examined after 48 hours. All the cells were collected and fixed with 4% paraformaldehyde and stained with 0.1% crystal violet. A cotton swab was used to remove non-migrated cells, and the images from five random fields at 200 \times magnification were captured by a microscope, and the number of cells was counted.

Statistics analysis

SPSS (version 25.0) software was used for the statistical analysis. An unpaired, two-tailed Student's *t*-test was used to compare data between the two groups. Chi-square and rank-sum tests were used to analyze the relationship between FOXP3 expression levels and clinical characteristics. The Kaplan-Meier method was used for the survival analysis, and the unstratified log-rank test was adopted for comparison. A Cox proportional hazards model was used to estimate the HR of each clinicopathological variable for OS. All predictors with a P value <0.05 in the univariate Cox analyses were used in the multivariate analysis. P values were two-tailed, and P<0.05 was considered to be statistically significant.

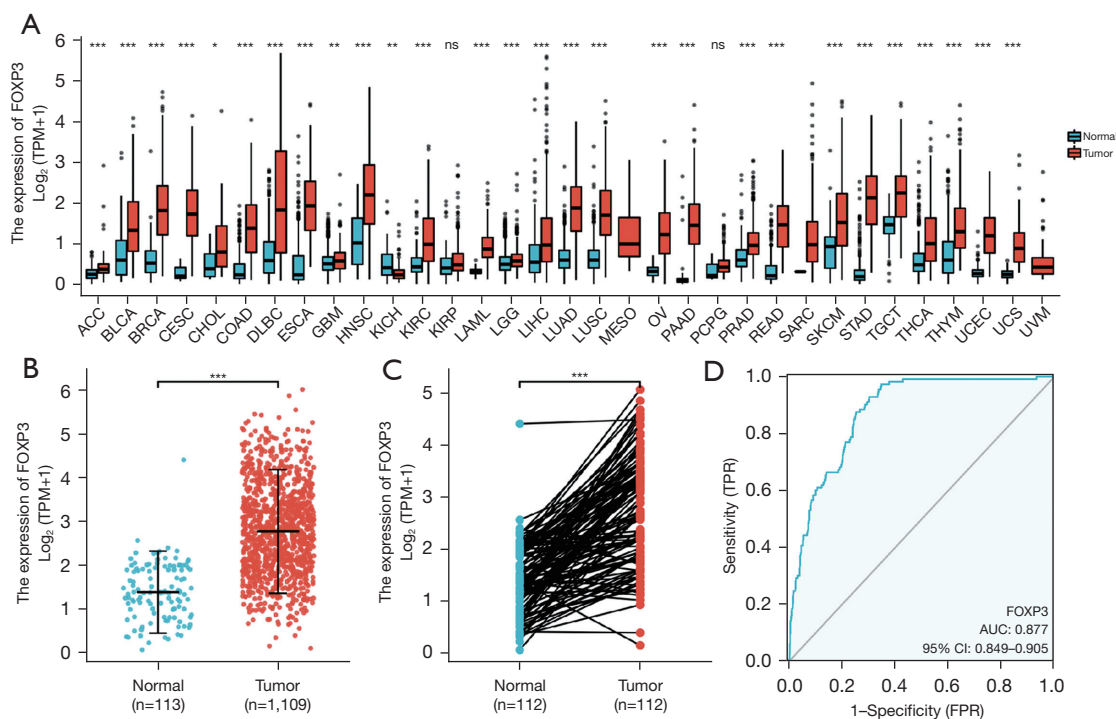


Figure 1 FOXP3 expression in BRCA and other types of human cancer from TCGA data. (A) FOXP3 expression levels in different tumor types from TCGA database; (B) expression levels of FOXP3 mRNA in BRCA (n=1,109) and normal tissues (n=113); (C) the expression of FOXP3 in BRCA (n=112) and its paired adjacent tissues (n=112); (D) ROC curve analysis of FOXP3 in BRCA (n=1,109). *, $P < 0.05$; **, $P < 0.01$; ***, $P < 0.001$; ns, no significance; BRCA, breast carcinoma; TCGA, the cancer genome atlas; ROC, receiver operating characteristic.

Results

FOXP3 expression and its diagnostic value in BRCA

To evaluate FOXP3 expression in human cancers, we searched FOXP3 mRNA expressions across 33 different types of tumors using RNA-seq data from TCGA. Our results showed that FOXP3 mRNA was highly expressed in 27 tumor types (Figure 1A). FOXP3 mRNA expression was significantly higher in the BRCA tumor group compared to the normal group among total (2.808 ± 1.020 vs. 1.409 ± 0.656 ; $P < 0.001$; Figure 1B) and paired specimens (2.784 ± 1.070 vs. 1.409 ± 0.659 ; $P < 0.001$; Figure 1C). Given the differential expression of FOXP3, we used normal and BC data to generate a ROC curve to further analyze the diagnostic value of FOXP3 in BRCA. The result indicated that the AUC of the ROC was 0.877 (95% CI: 0.849–0.905; Figure 1D), and the best cut-off value for FOXP3 was 2.171 (TPM). It revealed that FOXP3 had good diagnostic accuracy in distinguishing BRCA from normal controls.

In addition, FOXP3 mRNA expression was strongly correlated with ER/PR negative expression (Figure 2A,2B)

and early T1 classification ($P < 0.05$, Figure 2C), whereas no significant associations were found with HER2 status ($P = 0.051$, Figure 2D) or TNM stage ($P = 0.482$, Figure 2E). FOXP3 expression was significantly associated with molecular subtypes ($P < 0.001$) and displayed the highest ratio in the HER2+ BRCA subtype (Figure 2F).

Prognostic analysis of FOXP3 expression in BRCA

We used the Kaplan-Meier plotter database, PrognoScan database, and TCGA BRCA database to assess the relationship between FOXP3 expression and the prognosis of BRCA patients. The Kaplan-Meier plotter showed that BRCA patients with a high FOXP3 expression had a better RFS (HR = 0.74, 95% CI: 0.63–0.88, $P < 0.001$; Figure 3A) and OS (HR = 0.75, 95% CI: 0.56–0.99, $P = 0.041$; Figure 3B) than patients in the low FOXP3 expression group. Additionally, TCGA BRCA database also suggested that high FOXP3 expression was associated with a favorable OS in the basal-like (HR = 0.61, 95% CI: 0.38–0.99, $P = 0.042$; Figure 3C) and HER2+ (HR = 0.41, 95% CI: 0.17–0.98,

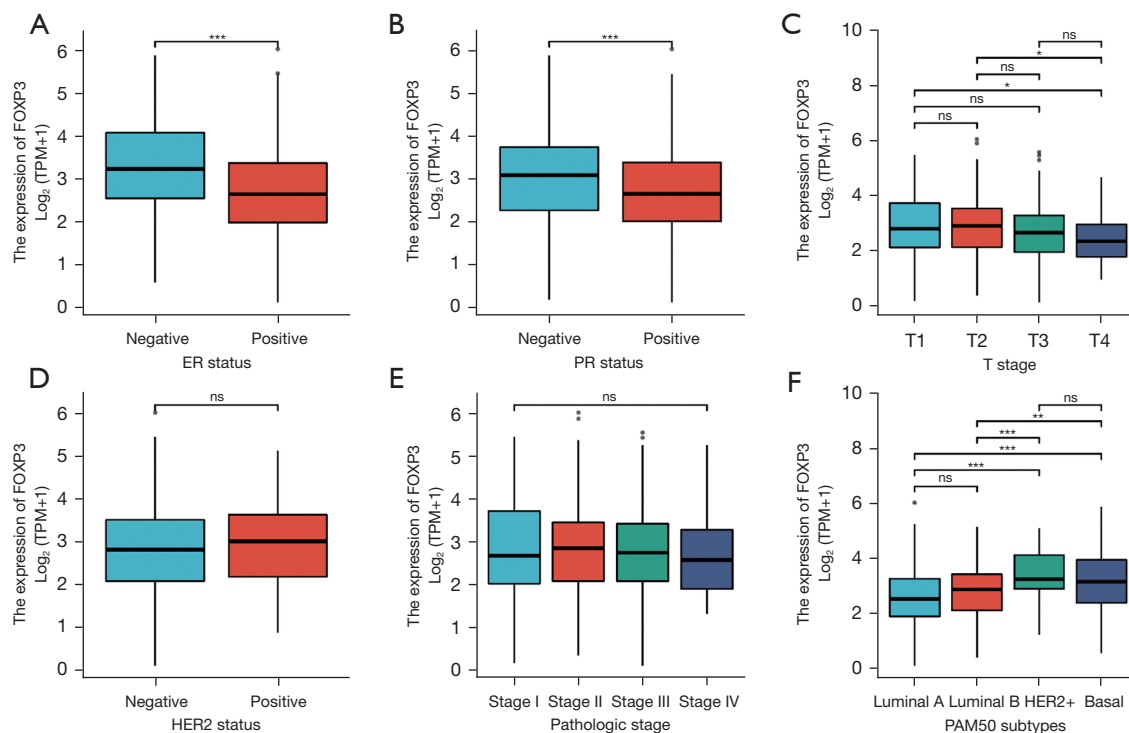


Figure 2 FOXP3 expression in BRCA based on different characteristics from TCGA data. (A) The association of FOXP3 expression and ER status in BRCA (n=485); (B) the association of FOXP3 expression and PR status in BRCA (n=478); (C) the association of FOXP3 expression and T classification in BRCA (n=498); (D) the association of FOXP3 expression and HER2 status in BRCA (n=486); (E) the association of FOXP3 expression and pathologic TNM stage classifications in BRCA (n=498); (F) the association of FOXP3 expression and different subtypes in BRCA (n=481). *, $P < 0.05$, **, $P < 0.01$, and ***, $P < 0.001$; ns, no significance; BRCA, breast carcinoma; TCGA, the cancer genome atlas; ER, estrogen receptor; PR, progesterone receptor; HER2, human epidermal growth factor receptor 2; TNBC, triple-negative breast cancer.

$P = 0.033$; *Figure 3D*) subtypes of BRCA patients. However, there was no significant difference between the expression of FOXP3 and the prognosis of HER2 negative BRCA patients (HR =1.25, 95% CI: 0.75–2.08, $P = 0.0393$; *Figure 3E*). Moreover, we used GSE2034 data from the GEO databases in PrognScan to further verify the effect of FOXP3 on the survival of BRCA patients. The result demonstrated the same favorable outcome for distant metastasis-free survival (DMFS) (HR =0.76, 95% CI: 0.57–1.00, $P = 0.0495$; *Figure 3F*) in BRCA patients with a high FOXP3 expression.

Genomic alterations and methylation pattern of FOXP3 in BRCA

To further verify the mechanism underlying the differential expression levels of FOXP3 in BRCA and normal tissues, we used the cBio-Portal database to analyze the association

between FOXP3 mRNA expression and its genome status. Firstly, we selected the pan-cancer data for analysis (*Figure 4A*), which showed a relatively lower alteration frequency of the FOXP3 genome in BRCA cases, including mutation, amplification (AMP), and deep deletion. Subsequently, we focused on the eight BRCA studies in TCGA data (*Figure 4B*). The highest mutation rate of FOXP3 was 1.64% (2/122 cases) in study 1 (proteogenomic landscape of breast cancer, CPTAC, Cell 2020). AMP was the most common alteration in study 3 (1.18%, 13/1,099) (invasive BRCA, TCGA, Firehose Legacy). The highest frequency of deep deletion was only 0.24% (2/817) in study 2 (invasive BRCA, TCGA, Cell 2015). Overall, the alteration frequency of the FOXP3 genome was not prominent in BRCA. Moreover, it demonstrated that CNV made no difference to FOXP3 mRNA expression (*Figure 4C*) or BRCA prognosis (log-rank $P = 0.210$)

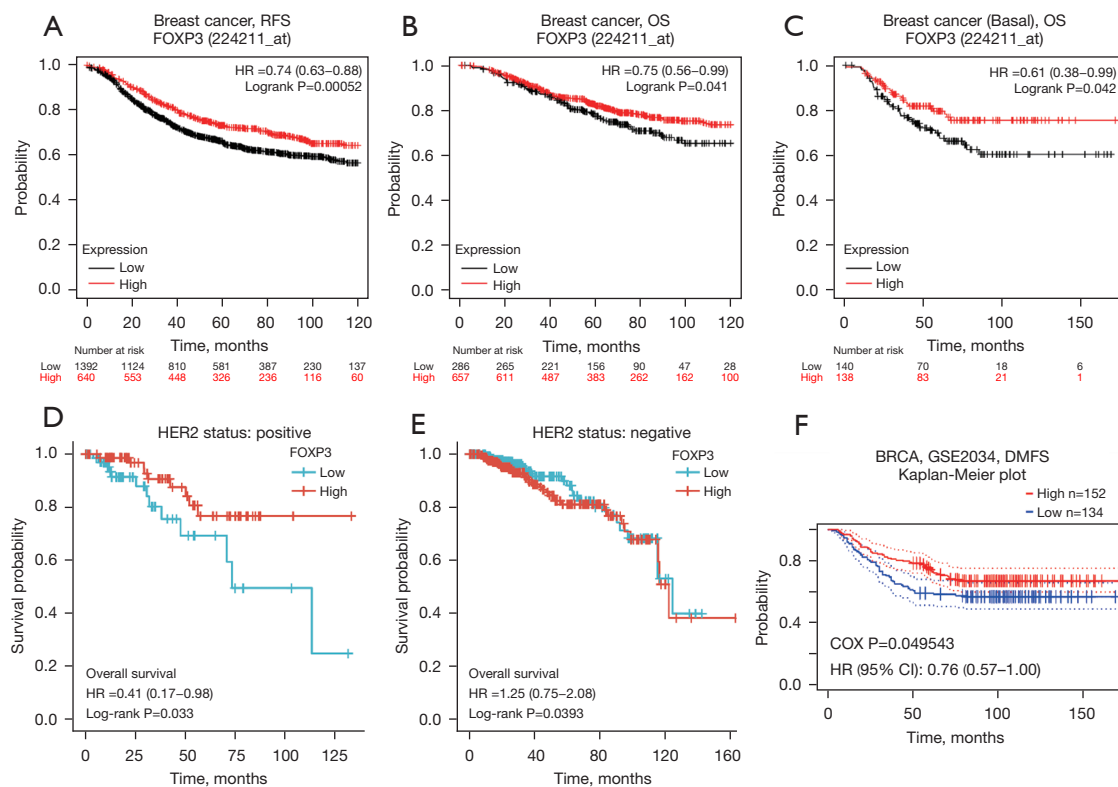


Figure 3 The prognostic value of FOXP3 expression in BRCA. (A) RFS survival curves of breast cancer in the Kaplan-Meier plotter database (n=2,032); (B) OS survival curves of breast cancer in the Kaplan-Meier plotter database (n=943); (C) OS survival curves of basal-like breast cancer in the Kaplan-Meier plotter database (n=278); (D) OS survival curves of breast cancer with HER2 positive status (n=157) from TCGA data; (E) OS survival curves of breast cancer with HER2 negative status from TCGA data (n=558); (F) DMFS survival curves of breast cancer from GSE 2034 data (n=286). BRCA, breast carcinoma; RFS, relapse-free survival; OS, overall survival; TCGA, the cancer genome atlas; HER2, human epidermal growth factor receptor 2; DMFS, distant metastasis-free survival.

(Figure 4D). This suggested that genomic alterations may not be the main cause of FOXP3 high expression and its prognostic value.

Furthermore, we analyzed the relationship between FOXP3 methylation and gene expression. The results from the UALCAN database showed that FOXP3 was highly expressed in BRCA tumor tissues compared with normal tissues ($P < 0.001$; Figure 5A). Conversely, the gene promoter methylation of FOXP3 in the tumor tissues of TCGA-BRCA was significantly lower than that of adjacent normal tissues ($P < 0.001$; Figure 5B). This suggested that the level of FOXP3 promoter methylation was negatively correlated with FOXP3 expression (Spearman Cor = -0.133 , $P < 0.001$, Figure 5C). In addition, the MethSurv analyses demonstrated that BRCA patients with FOXP3 hypomethylation in TSS200-open-sea-cg04920616 (HR = 1.596, $P = 0.03$) and 5'UTR-open-sea-cg10858077 (HR

= 1.867, $P = 0.005$) located in CpG island, and body-open-sea-cg06767008 (HR = 1.566, $P = 0.043$) were associated with a favorable prognosis (Figure 5D, 5E).

FOXP3 coexpression gene and pathway enrichment in BRCA

To clarify the potential antitumor mechanism of FOXP3 in BRCA, we next enriched the coexpression gene pathways to visualize the connection between FOXP3 and its DEGs. The FOXP3-associated DEGs from TCGA BRCA database are shown in the volcano map (Figure 6A). A total of 698 DEGs with $|\log_2(\text{FC})| > 2$ and $P_{\text{adj}} < 0.05$ were identified, of which 490 genes were upregulated and 208 were downregulated. The protein-protein interaction (PPI) network of the top DEGs with significant correlations with FOXP3 is shown in Figure 6B. In addition, we performed

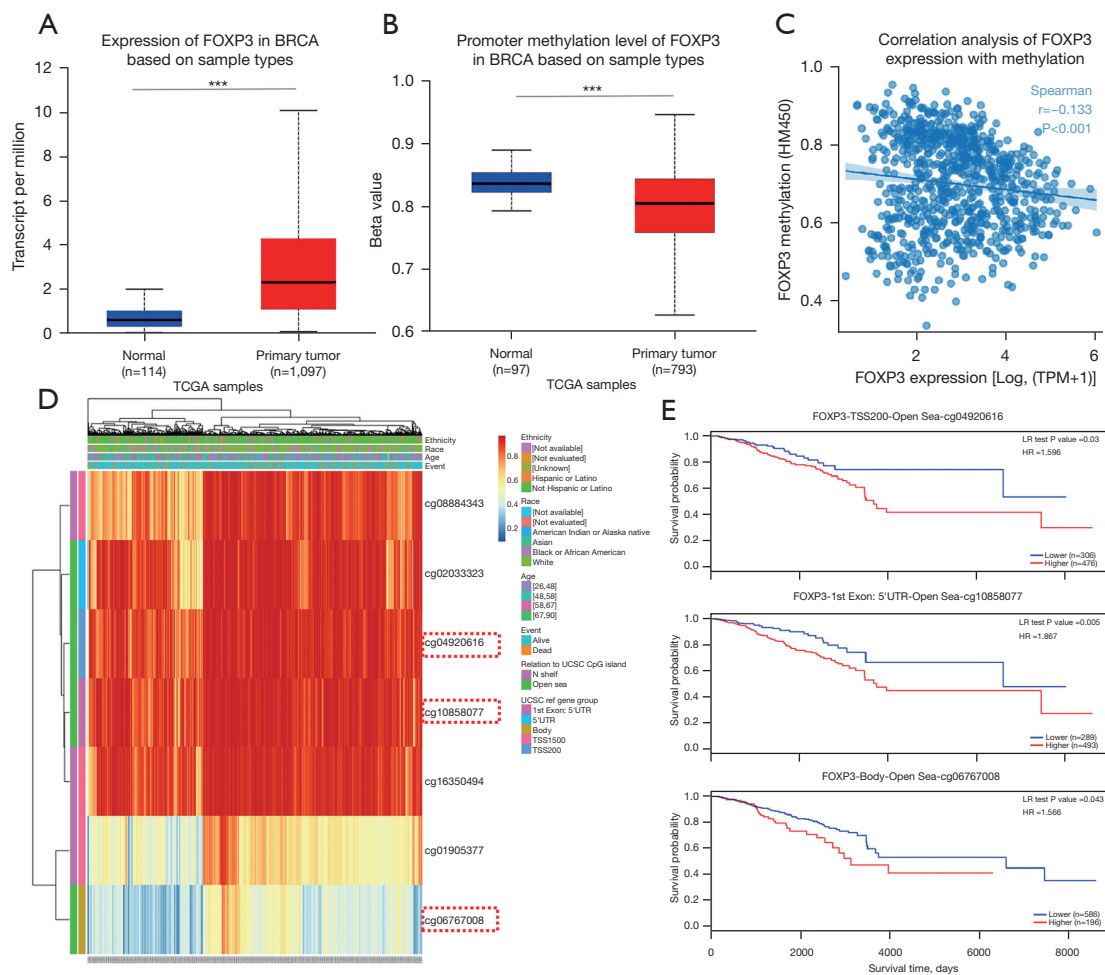


Figure 5 FOXP3 expression and methylation pattern in BRCA. (A) FOXP3 expression in BRCA and normal tissue from UALCAN; (B) FOXP3 promoter methylation level in BRCA and normal tissues from UALCAN; (C) correlation analysis of FOXP3 mRNA expression with FOXP3 promoter methylation status; (D) the visualization heat map of DNA methylation at CpG sites of the FOXP3 gene in BRCA from MethSurv data; (E) the Kaplan-Meier survival analysis of the promoter methylation of FOXP3 in BRCA from MethSurv data. ***, $P < 0.001$. BRCA, breast carcinoma.

protein in BRCA, immunohistochemistry (IHC) staining was performed on 123 BRCA and 20 benign breast fibroadenoma tissues from our clinical specimen bank. As shown in *Figure 7A-7D*, we found that FOXP3 exhibited a heterogeneous subcellular location in both the tumor nucleus and cytoplasm of BRCA instead of being mainly located in the nucleus in Treg. It is noteworthy that only nuclear staining was defined as positive for FOXP3 in our study based on its transcription factor value (21), and staining of at least 25% of the nucleus was considered a high FOXP3 expression (22). By comparison, FOXP3 positive staining was not detected in benign breast fibroadenoma tissues. In our series, high and low FOXP3

expression was 48.0% (59/123) and 52.0% (64/123) in BRCA tissues, respectively. In addition, FOXP3 protein expression was higher in the negative vessel tumor embolus group compared with the positive vessel tumor embolus group (54.7% vs. 32.4%, $P = 0.024$). Also, FOXP3 expression was significantly associated with low Ki67 status (61.5% vs. 41.7%, $P = 0.041$) (*Table 1*).

Furthermore, the KM survival analysis demonstrated that high expression of FOXP3 was significantly associated with favorable OS in the total BRCA population (10-year survival probability, 88.1% vs. 73.4%; log-rank $P = 0.035$; *Figure 7E*) and TNBC patients (10-year survival probability, 84.6% vs. 41.7%; log-rank $P = 0.015$; *Figure 7F*), but it did

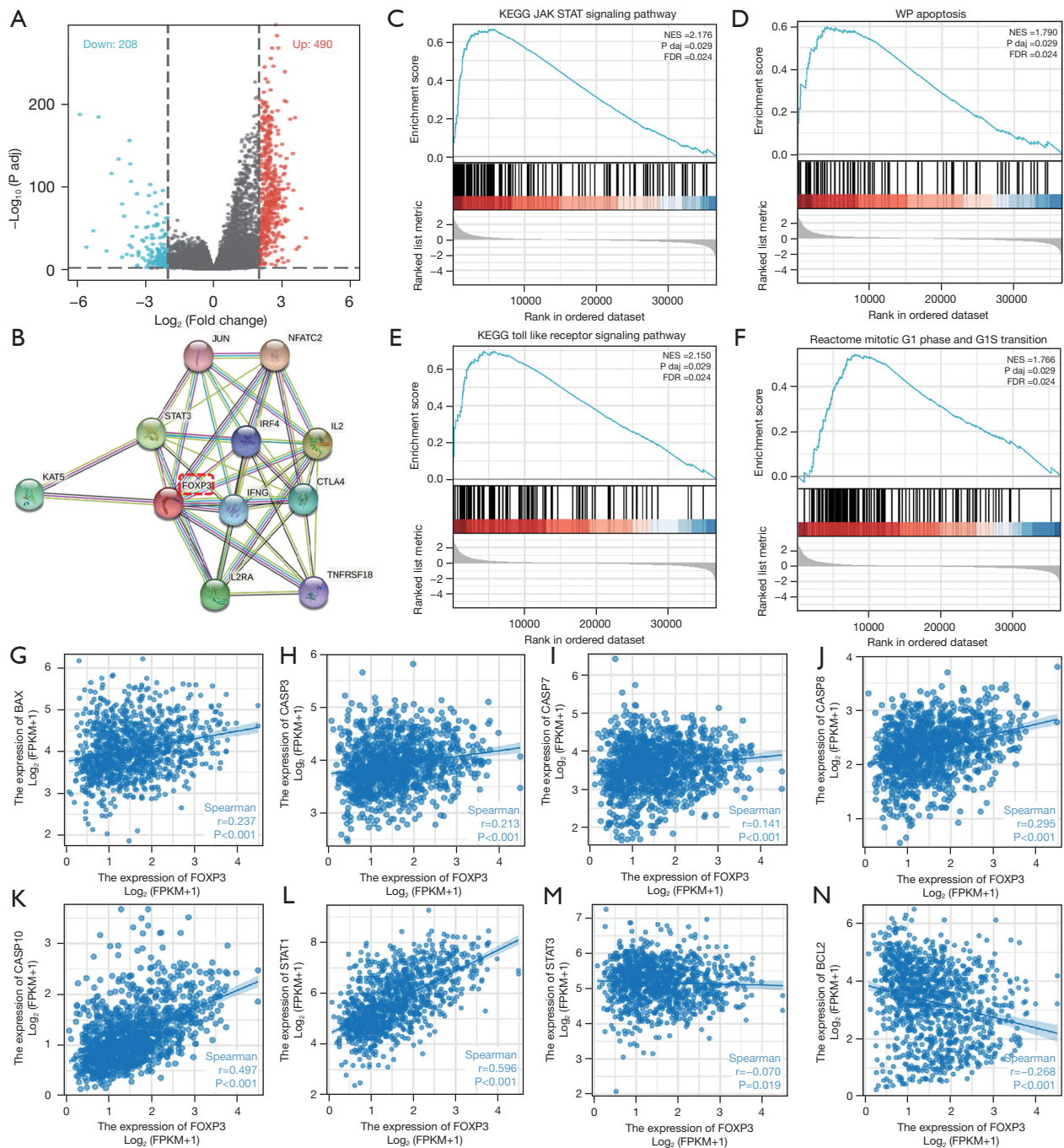


Figure 6 FOXP3 coexpression gene and pathway enrichment in BRCA. (A) Volcano plot of FOXP3-associated DEGs in TCGA BRCA database; (B) the PPI network of the top FOXP3 DEGs; (C-F) GSEA functional enrichment of FOXP3 associated DEGs in BRCA; (C) KEGG JAK-STAT signaling pathway; (D) WP apoptosis; (E) KEGG Toll-like receptor signaling pathway; (F) REACTOME Mitotic G1 phase and G1/S transition; (G-N) the correlation analyses of FOXP3 expression with related genes: (G) FOXP3 with pro-apoptotic protein BAX; (H) FOXP3 with Caspase 3; (I) FOXP3 with Caspase 7; (J) FOXP3 with Caspase 8; (K) FOXP3 with Caspase 10; (L) FOXP3 with antioncogene STAT1; (M) FOXP3 with cancer-promoting gene STAT3; (N) FOXP3 with anti-apoptotic protein BCL2. BRCA, breast carcinoma; DEGs, differentially expressed genes; TCGA, The Cancer Genome Atlas; PPI, protein-protein interaction.

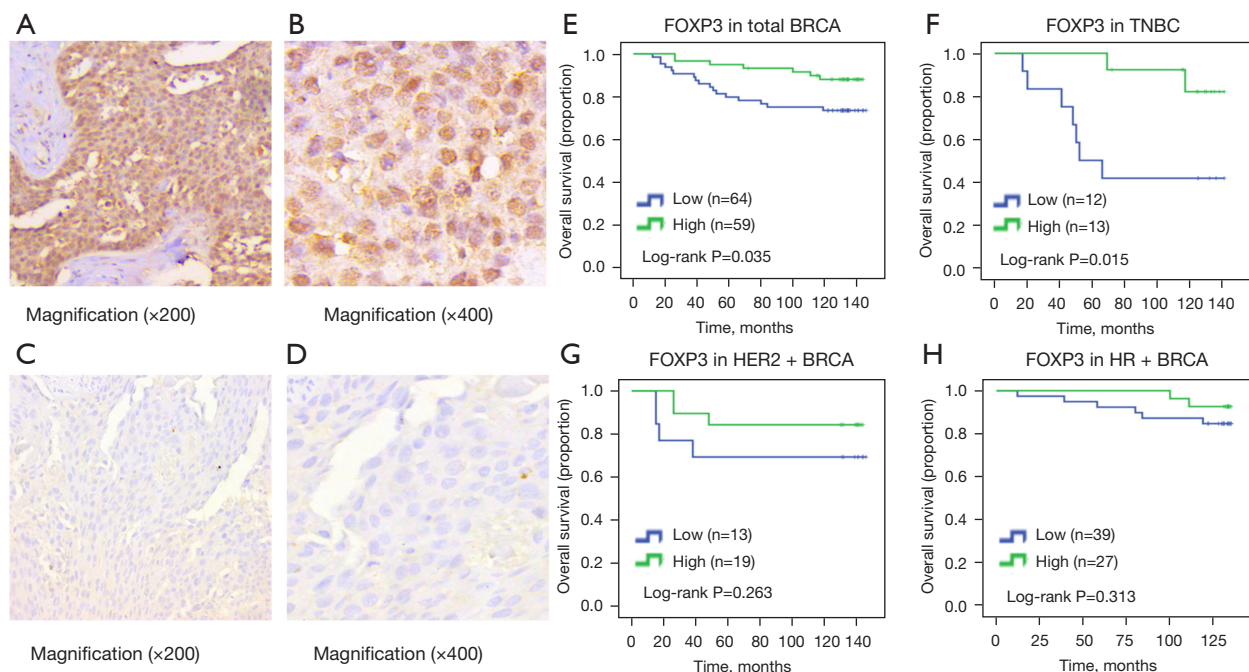


Figure 7 FOXP3 protein expression and its prognostic value in our BRCA tissues. (A-D) Representative IHC staining patterns of FOXP3 in BRCA tissues: (A) positive, magnification ($\times 200$), (B) positive, magnification ($\times 400$), (C) negative, magnification ($\times 200$), (D) negative, magnification ($\times 400$). (E) OS rate of FOXP3 in total BRCA patients (n=123). (F) OS rate of FOXP3 in TNBC patients (n=25). (G) OS rate of FOXP3 in HER2+ BRCA patients (n=32). (H) OS rate of FOXP3 in HR+ BRCA patients (n=66). BRCA, breast carcinoma; IHC, immunohistochemistry; BRCA, breast carcinoma; OS, overall survival; TNBC, triple-negative breast cancer; HER2, human epidermal growth factor receptor 2; HR, hormone receptor.

not reach statistical difference in HER2+ (10-year survival probability, 84.2% vs. 69.2%; log-rank $P=0.263$; Figure 7G) or HR+ BRCA patients (10-year survival probability, 92.6% vs. 84.6%; log-rank $P=0.313$; Figure 7H). In addition, positive lymph node, T ≥ 2 cm, TNM stage III, and positive vessel tumor embolus were risks for OS (all HR >1 ; $P<0.05$) in the univariate Cox analysis (Table 2). Subsequently, all predictors with P values <0.05 in the univariate analyses were included in the multivariate Cox analysis (Table 2), which indicated that high FOXP3 expression (HR: 0.367; 95% CI: 0.144–0.935; $P=0.036$) and ER/PR positive (HR: 0.368; 95% CI: 0.144–0.938, $P=0.036$) were both independent protective factors for OS in BRCA.

Investigation of the biological function of FOXP3 in BRCA cell lines

FOXP3 mRNA expression data were detected in various cancer cell lines from the HPA database, demonstrating the highest expression level in the MCF-7 cell lines

of the female reproductive system (Figure 8A). As the immunofluorescence (IF) staining HPA045943 of the HPA database showed, FOXP3 protein was located in the nucleoplasm of MCF-7 cells (green staining, Figure 8B). Using quantitative real-time PCR, we validated FOXP3 mRNA expression in five types of common BRCA cell lines, including MCF-7, MDA-MB-231, MDA-MB-453, BT-474, and SK-BR-3. peripheral blood mononuclear cell (PBMC) with enriched lymph cells was regarded as the positive control cell. Consistently, the result showed that FOXP3 mRNA expression was highest in MCF-7 cell lines ($P<0.05$, Figure 8C). Therefore, the MCF-7 cell line was selected for the gene knockdown experiment by using small RNA interference technology to investigate the value of FOXP3 further. FOXP3 protein expression was significantly downregulated in si-FOXP3 cells compared with the si-NC and MCF-7 control groups detected by western blot (0.15 ± 0.03 vs. 1.02 ± 0.05 vs. 1.07 ± 0.09 ; $P<0.05$; Figure 8D–8E). As expected, migration and invasion assays showed that FOXP3 knockdown significantly enhanced

Table 2 Univariate and multivariate analyses (Cox regression) for OS (n=123)

Characteristics	Univariate analysis		Multivariate analysis	
	Hazard ratio (95% CI)	P	Hazard ratio (95% CI)	P
Positive lymph node	2.550 (1.091–5.961)	0.031	2.033 (0.688–6.001)	0.199
T ≥2 cm	2.753 (1.141–6.640)	0.024	1.924 (0.575–6.434)	0.288
TNM stage III	4.514 (1.128–18.060)	0.033	1.143 (0.161–8.115)	0.894
Vessel tumor embolus	2.438 (1.092–5.446)	0.030	1.774 (0.725–4.339)	0.209
ER/PR positive	0.371 (0.159–0.867)	0.022	0.368 (0.144–0.938)	0.036
High FOXP3 expression	0.400 (0.166–0.965)	0.042	0.367 (0.144–0.935)	0.036

OS, overall survival; CI, confidence interval; ER, estrogen receptor; PR, progesterone receptor.

migration (percent: 38.12%±3.87% vs. 18.76%±7.17% vs. 17.82%±8.61%; P<0.05; *Figure 8F*) and invasion (transmembrane cell number: 61.67±8.17 vs. 32.56±7.24 vs. 25.56±5.74; P<0.001; *Figure 8G*) abilities in si-FOXP3 cells compared with si-NC and MCF-7 control cells.

Discussion

FOXP3 is a key member of the FOX transcription factor family, which plays an important role in cell growth, proliferation, and differentiation (23). Although the value of FOXP3 was mainly focused on Treg cells in early research, recent evidence has indicated that its expression in tumor cells is associated with the progression of various cancers (8). In this study, we used RNA-seq data from TCGA and found that *FOXP3* mRNA was highly expressed in 27 types of tumor tissues. Similarly, FOXP3 expression was upregulated in BRCA compared with adjacent normal tissues. Meanwhile, the ROC curve showed that FOXP3 demonstrated significant diagnostic value as a potential diagnostic biomarker for BRCA. In addition, the high expression of FOXP3 predicted a favorable prognosis in BRCA patients, verified in various databases. This finding is in line with several *in vitro* studies demonstrating that FOXP3 inhibits the expression of proto-oncogene HER2 (10), RUNX1 (11), VEGF (12), MTA1 (13), CD44 (24), and CXCR4 (25) to perform its anticancer function in BRCA. Moreover, we validated the expression and prognostic value of nuclear FOXP3 in 123 BRCA samples. Notably, high FOXP3 expression was significantly associated with negative vessel tumor embolus and low Ki67 status. Nuclear FOXP3 expression was verified as an independent favorable factor for OS in BRCA, especially in TNBC. This finding is essentially consistent with recent studies (12,13).

However, in sharp contrast to a putative onco-suppressor role for FOXP3, some studies have revealed a correlation between FOXP3 expression and poor prognosis in BRCA (22,26,27). Contrary to our results, Kim *et al.* (27) found that FOXP3 expression in the nucleus and/or cytoplasm was related to a high Ki67 index and poor DFS in a node-positive subgroup. The primary reason for this discrepancy may be the positive definition of FOXP3 cytoplasm staining in their study. According to recent research, the ability of FOXP3 to enter the nucleus is a requirement for it to regulate downstream gene expression (7,8,21). In other words, FOXP3 would fail to function properly as a transcription factor when trapped in the cytoplasm. Therefore, only samples with nuclear staining were defined as positive for FOXP3 expression in our study and consequently displayed its anticancer capability in BRCA.

Based on the results above, FOXP3 was identified as highly expressed in BRCA and a tumor suppressor gene. Subsequently, we explored the mechanism of FOXP3 upregulation in BRCA. Our results showed a negative correlation between FOXP3 mRNA levels and promoter methylation levels in the UALCAN database. DNA methylation is an essential type of chemical modification that can change genetic performance without changing the gene sequence, belonging to the epigenetic regulatory category in tumorigenesis (28). It is also intriguing to note that Tregs could not withstand CpG methylation, which transformed them into unstable regulatory phenotypes (29,30). The differentiation of Treg cells was mediated through the FOXP3 CpG hypomethylation pattern, which accounts for 70–80% of the genome (31). In our study, we demonstrated the hypomethylated state of FOXP3 promoter in BRCA. Conversely, most CpG sites are methylated in normal tissues (28). Given the negative correlation between the promoter methylation level and FOXP3 expression

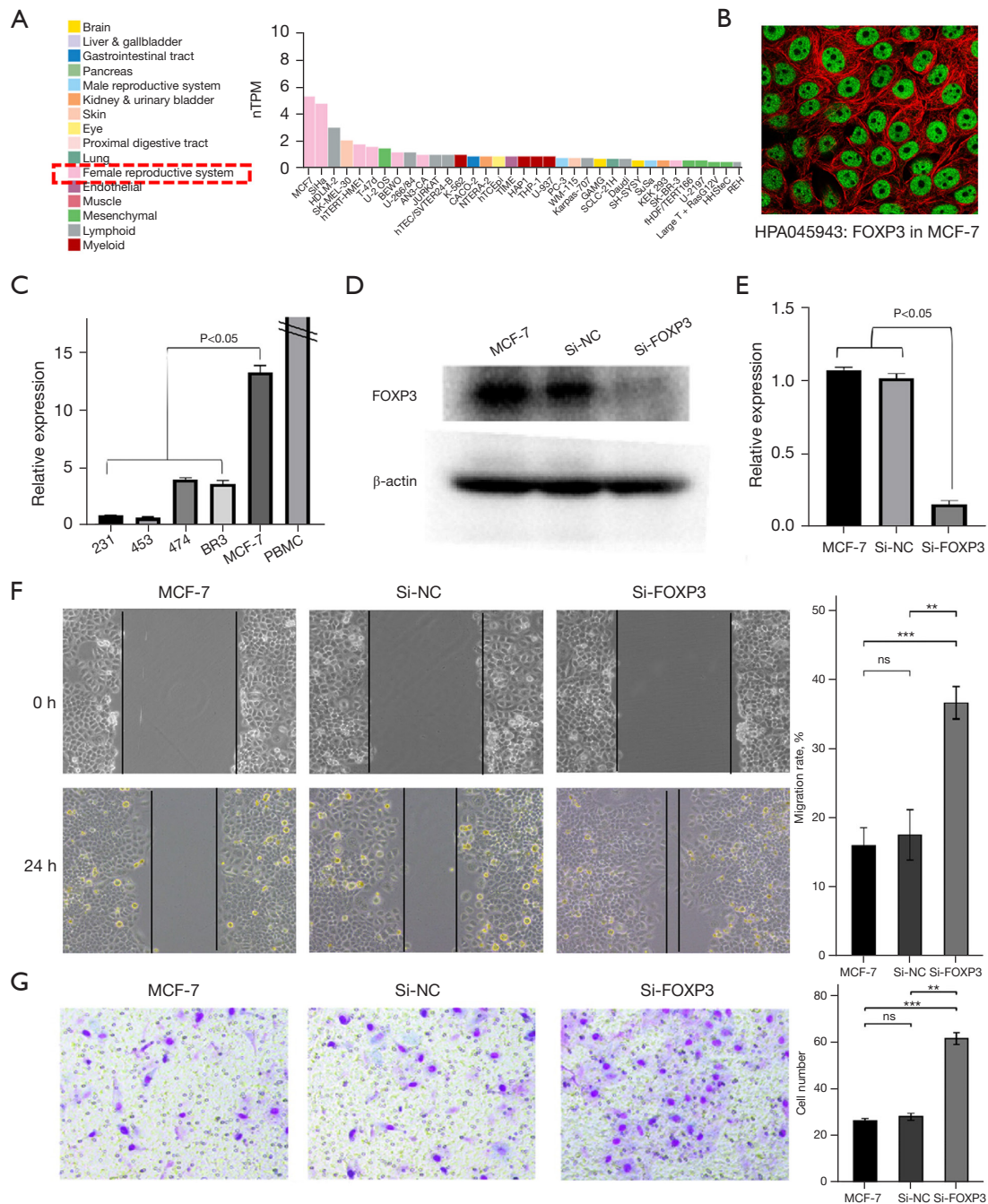


Figure 8 FOXP3 expression in cell lines. (A) FOXP3 mRNA expression data in various cancer cell lines from the HPA database; (B) FOXP3 protein located in the nucleoplasm of MCF-7 cells from the HPA database (IF, $\times 400$); (C) FOXP3 mRNA expression in MCF-7, MDA-MB-231, MDA-MB-453, BT-474, and SK-BR-3 BRCA cell lines. PBMC was regarded as the positive control; (D) FOXP3 protein expression decreased in MCF-7 transfected with FOXP3 siRNA by western blot; (E) FOXP3 mRNA expression decreased in MCF-7 transfected with FOXP3 siRNA by qRT-PCR; (F) FOXP3 knockdown enhanced the ability of MCF-7 cell migration evaluated by wound healing assay (microscope, $\times 100$); (G) FOXP3 knockdown enhanced the invasion ability of MCF-7 cell in transwell chamber stained with crystal violet (microscope, $\times 200$). **, $P < 0.01$, ***, $P < 0.001$. ns, no significance; qRT-PCR, quantitative real-time PCR; HPA, human protein atlas; IF, immunofluorescence; PBMC, peripheral blood mononuclear cell.

level, we speculated that FOXP3 promoter methylation would lead to transcriptional gene silencing in BRCA. In addition, we validated that BRCA patients with FOXP3 hypomethylation in TSS200-open-sea-cg04920616 and 5'UTR-open-sea-cg10858077 located in CpG islands and body-open-sea-cg06767008 were associated with a favorable prognosis in BRCA by the MethSurv analyses. In summary, a hypomethylated state of FOXP3 promoter may be a prerequisite for its high expression and anticancer activity in BRCA.

In addition, genome variations of FOXP3 may also influence its stable protein expression. Similar to some actively studied transcription factors, such as TP53, FOXP3 is mutated in some cancers, including hepatocellular carcinoma (32) and prostate cancer (33). However, we found an extremely lower overall alteration frequency of the FOXP3 genome in BRCA. In addition, CNV demonstrated no correlation to the FOXP3 mRNA expression and BRCA prognosis. A recent study detected transcriptional mutations in the forkhead (FKH) domain of FOXP3 mRNA in 33% of HCC tumor tissues (32), which caused the delocalization of FOXP3 from the nucleus to the cytoplasm (34) and was associated with a worse prognosis in HCC patients. In another study, cytoplasm FOXP3 also demonstrated the existence of mutant FOXP3 proteins with altered FKH domains in BRCA (22). More research is needed to further understand the complex genome variation and its biological value in FOXP3.

As a transcription factor, FOXP3 may regulate specific target genes in the biological processes of tumor development, but the precise mechanisms have not been fully illustrated. In our attempt to better understand FOXP3's inhibitory effect on BRCA, we enriched the potential pathways of FOXP3 coexpressed genes in BRCA through GSEA analysis. We found that FOXP3 was mainly involved in the JAK/STAT signaling pathway, Toll-like receptor (TLR) signaling pathway, cell cycle, and apoptosis process in BRCA. These were consistent with previous studies. FOXP3 was reported to be involved in the TLR-NF- κ B signaling pathway in autoimmune diseases (35). Recently, it was demonstrated that FOXP3 DEGs were enriched in the TLR signaling pathway in colorectal cancer (36). The IL-10/JAK/STAT signaling pathway also played an important modulating role in FOXP3-expressing T cell neoplasms and several inflammatory diseases (37). Lan *et al.* demonstrated that FOXP3 might be related to pSTAT3 expression in patients with chronic rhinosinusitis with nasal polyps (38). In terms of the cell cycle process, Matoba

et al. revealed that FOXP3+ Treg cells with abundant surface expression of CTLA-4 have a gene expression profile correlating to cell cycle, cell proliferation, and DNA replication in human head and neck cancer tissues (39). Ostrow *et al.* identified FKH1 and FKH2 FOX proteins as necessary for the clustering of a subset of replication origins in the G₁ phase and the early initiation of these origins in the ensuing S phase in *Saccharomyces cerevisiae* (40). Our *in vitro* study found that FOXP3 knockdown promoted migration and invasion of MCF-7 cell lines. However, it is not sufficient to definitively clarify the molecular mechanism of FOXP3. The signaling pathways of FOXP3 need further *in vitro* and *in vivo* studies to provide validation in BRCA.

In this study, we used a variety of databases to explore the expression, prognosis, genomic variation, methylation status, and enriched pathways of FOXP3 in BRCA. We found that FOXP3 was highly expressed in BRCA and may be a potential diagnostic biomarker. Moreover, promoter hypomethylation and upregulation of FOXP3 expression were favorable for the prognosis of BRCA. Therefore, FOXP3 is considered a tumor-associated biomarker and has value as a possible target for BRCA therapy in the future. But further research is necessary. Although this study improved our understanding of the relationship between FOXP3 and BRCA, there were some limitations. First, the main limitation of the study is the lack of discrimination in the different gene expression profiles in single-cell populations from the TCGA and other dataset repositories. From these RNA-seq data, it is not possible to separate the gene expression of FOXP3+ tumor cells from FOXP3+ Tregs. Further single-cell RNA sequencing technology and spatial-profiling-based approaches may help overcome this problem by individually investigating the biological value of FOXP3 in BRCA cells. Second, further comprehensive research is necessary to verify the genomic alterations in the DNA, mRNA, and protein levels of FOXP3 in BRCA. Third, the *in vitro* migration and invasion functions still need to be validated by *in vivo* animal metastasis models. Furthermore, these critical signaling pathways involved in tumor progression should be verified further by *in vitro* and *in vivo* experiences, as additional relevant pathways may have been missed in our study.

In conclusion, this study demonstrated that FOXP3 has a prognostic and diagnostic value for BRCA. We provided evidence that the high expression and promoter hypomethylation of FOXP3 were both related to a favorable OS in BRCA patients. Moreover, exploring FOXP3-related pathways provided important clues for its biological

mechanism in BRCA by regulating the tumor progression, cell cycle, and apoptosis. This study demonstrated FOXP3 to be a novel biomarker for the diagnosis and prognosis of BRCA and a potential candidate target for BRCA treatment, expecting to provide a new direction for clinical diagnosis and treatment in BRCA.

Acknowledgments

Funding: This study was supported by the Livelihood Technology Special Project in the Key Project of Hebei Province (No. 192777125D).

Footnote

Reporting Checklist: The authors have completed the REMARK reporting checklist. Available at <https://atm.amegroups.com/article/view/10.21037/atm-22-3080/rc>

Data Sharing Statement: Available at <https://atm.amegroups.com/article/view/10.21037/atm-22-3080/dss>

Conflicts of Interest: All authors have completed the ICMJE uniform disclosure form (available at <https://atm.amegroups.com/article/view/10.21037/atm-22-3080/coif>). The authors have no conflicts of interest to declare.

Ethical Statement: The authors are accountable for all aspects of the work in ensuring that questions related to the accuracy or integrity of any part of the work are appropriately investigated and resolved. The study was conducted in accordance with the Declaration of Helsinki (as revised in 2013). The study was approved by institutional ethics committee of the Fourth Hospital of Hebei Medical University (No. 2018MEC116). Informed consent was taken from all the patients.

Open Access Statement: This is an Open Access article distributed in accordance with the Creative Commons Attribution-NonCommercial-NoDerivs 4.0 International License (CC BY-NC-ND 4.0), which permits the non-commercial replication and distribution of the article with the strict proviso that no changes or edits are made and the original work is properly cited (including links to both the formal publication through the relevant DOI and the license). See: <https://creativecommons.org/licenses/by-nc-nd/4.0/>.

References

1. Sung H, Ferlay J, Siegel RL, et al. Global Cancer Statistics 2020: GLOBOCAN Estimates of Incidence and Mortality Worldwide for 36 Cancers in 185 Countries. *CA Cancer J Clin* 2021;71:209-49.
2. Britt KL, Cuzick J, Phillips KA. Key steps for effective breast cancer prevention. *Nat Rev Cancer* 2020;20:417-36.
3. Grinda T, Antoine A, Jacot W, et al. Evolution of overall survival and receipt of new therapies by subtype among 20446 metastatic breast cancer patients in the 2008-2017 ESME cohort. *ESMO Open* 2021;6:100114.
4. Ueno T. Biomarkers of neoadjuvant/adjuvant endocrine therapy for ER-positive/HER2-negative breast cancer. *Chin Clin Oncol* 2020;9:35.
5. Liang Y, Zhang H, Song X, et al. Metastatic heterogeneity of breast cancer: Molecular mechanism and potential therapeutic targets. *Semin Cancer Biol* 2020;60:14-27.
6. Qiu R, Zhou L, Ma Y, et al. Regulatory T Cell Plasticity and Stability and Autoimmune Diseases. *Clin Rev Allergy Immunol* 2020;58:52-70.
7. Ramsdell F, Rudensky AY. Foxp3: a genetic foundation for regulatory T cell differentiation and function. *Nat Immunol* 2020;21:708-9.
8. Jia H, Qi H, Gong Z, et al. The expression of FOXP3 and its role in human cancers. *Biochim Biophys Acta Rev Cancer* 2019;1871:170-8.
9. Yi J, Tan S, Zeng Y. et al. Comprehensive Analysis of Prognostic and immune infiltrates for FOXP3 Transcription Factors in Human Breast Cancer. *Sci Rep*, 2022, 12: 8896..
10. Zuo T, Wang L, Morrison C, et al. FOXP3 is an X-linked breast cancer suppressor gene and an important repressor of the HER-2/ErbB2 oncogene. *Cell* 2007;129:1275-86.
11. Recouvreux MS, Grasso EN, Echeverria PC, et al. RUNX1 and FOXP3 interplay regulates expression of breast cancer related genes. *Oncotarget* 2016;7:6552-65.
12. Li X, Gao Y, Li J, et al. FOXP3 inhibits angiogenesis by downregulating VEGF in breast cancer. *Cell Death Dis* 2018;9:744.
13. Liu C, Han J, Li X, et al. FOXP3 Inhibits the Metastasis of Breast Cancer by Downregulating the Expression of MTA1. *Front Oncol* 2021;11:656190.
14. Györfy B, Lanczky A, Eklund AC, et al. An online survival analysis tool to rapidly assess the effect of 22,277 genes on breast cancer prognosis using microarray data of 1,809 patients. *Breast Cancer Res Treat* 2010;123:725-31.

15. Chandrashekar DS, Bashel B, Balasubramanya SAH, et al. UALCAN: A Portal for Facilitating Tumor Subgroup Gene Expression and Survival Analyses. *Neoplasia* 2017;19:649-58.
16. Modhukur V, Iljasenko T, Metsalu T, et al. MethSurv: a web tool to perform multivariable survival analysis using DNA methylation data. *Epigenomics* 2018;10:277-88.
17. Cerami E, Gao J, Dogrusoz U, et al. The cBio cancer genomics portal: an open platform for exploring multidimensional cancer genomics data. *Cancer Discov* 2012;2:401-4.
18. Ritchie ME, Phipson B, Wu D, et al. limma powers differential expression analyses for RNA-sequencing and microarray studies. *Nucleic Acids Res* 2015;43:e47.
19. Subramanian A, Tamayo P, Mootha VK, et al. Gene set enrichment analysis: a knowledge-based approach for interpreting genome-wide expression profiles. *Proc Natl Acad Sci U S A* 2005;102:15545-50.
20. Uhlén M, Fagerberg L, Hallström BM, et al. Proteomics. Tissue-based map of the human proteome. *Science* 2015;347:1260419.
21. Chandra A, Goldman N, Vahedi G. Foxp3 Re-distributes Its Heavy Lifting. *Immunity* 2020;53:895-7.
22. Merlo A, Casalini P, Carcangiu ML, et al. FOXP3 expression and overall survival in breast cancer. *J Clin Oncol* 2009;27:1746-52.
23. Lam EW, Brosens JJ, Gomes AR, et al. Forkhead box proteins: tuning forks for transcriptional harmony. *Nat Rev Cancer* 2013;13:482-95.
24. Zhang C, Xu Y, Hao Q, et al. FOXP3 suppresses breast cancer metastasis through downregulation of CD44. *Int J Cancer* 2015;137:1279-90.
25. Douglass S, Meeson AP, Overbeck-Zubrzycka D, et al. Breast cancer metastasis: demonstration that FOXP3 regulates CXCR4 expression and the response to CXCL12. *J Pathol* 2014;234:74-85.
26. Won KY, Kim HS, Sung JY, et al. Tumoral FOXP3 has potential oncogenic function in conjunction with the p53 tumor suppressor protein and infiltrated Tregs in human breast carcinomas. *Pathol Res Pract* 2013;209:767-73.
27. Kim MH, Koo JS, Lee S. FOXP3 expression is related to high Ki-67 index and poor prognosis in lymph node-positive breast cancer patients. *Oncology* 2013;85:128-36.
28. Skvortsova K, Storzaker C, Taberlay P. The DNA methylation landscape in cancer. *Essays Biochem* 2019;63:797-811.
29. Morikawa H, Sakaguchi S. Genetic and epigenetic basis of Treg cell development and function: from a FoxP3-centered view to an epigenome-defined view of natural Treg cells. *Immunol Rev* 2014;259:192-205.
30. Morikawa H, Ohkura N, Vandenbon A, et al. Differential roles of epigenetic changes and Foxp3 expression in regulatory T cell-specific transcriptional regulation. *Proc Natl Acad Sci U S A* 2014;111:5289-94.
31. Smiline Girija AS. Protean role of epigenetic mechanisms and their impact in regulating the Tregs in TME. *Cancer Gene Ther* 2022;29:661-4.
32. Ren J, Liu Y, Wang S, et al. The FKH domain in FOXP3 mRNA frequently contains mutations in hepatocellular carcinoma that influence the subcellular localization and functions of FOXP3. *J Biol Chem* 2020;295:5484-95.
33. Wang L, Liu R, Li W, et al. Somatic single hits inactivate the X-linked tumor suppressor FOXP3 in the prostate. *Cancer Cell* 2009;16:336-46.
34. Vermulst M, Denney AS, Lang MJ, et al. Transcription errors induce proteotoxic stress and shorten cellular lifespan. *Nat Commun* 2015;6:8065.
35. Xu Y, Liu E, Xie X, et al. Induction of Foxp3 and activation of Tregs by HSP gp96 for treatment of autoimmune diseases. *iScience* 2021;24:103445.
36. Jacob S, Jurinovic V, Lampert C, et al. The association of immunosurveillance and distant metastases in colorectal cancer. *J Cancer Res Clin Oncol* 2021;147:3333-41.
37. Higuchi Y, Yasunaga JI, Mitagami Y, et al. HTLV-1 induces T cell malignancy and inflammation by viral antisense factor-mediated modulation of the cytokine signaling. *Proc Natl Acad Sci U S A* 2020;117:13740-9.
38. Lan F, Zhang N, Zhang J, et al. Forkhead box protein 3 in human nasal polyp regulatory T cells is regulated by the protein suppressor of cytokine signaling 3. *J Allergy Clin Immunol* 2013;132:1314-21.
39. Matoba T, Imai M, Ohkura N, et al. Regulatory T cells expressing abundant CTLA-4 on the cell surface with a proliferative gene profile are key features of human head and neck cancer. *Int J Cancer* 2019;144:2811-22.
40. Ostrow AZ, Kalhor R, Gan Y, et al. Conserved forkhead dimerization motif controls DNA replication timing and spatial organization of chromosomes in *S. cerevisiae*. *Proc Natl Acad Sci U S A* 2017;114:E2411-9.

Cite this article as: Li J, Zhang X, Liu B, Shi C, Ma X, Ren S, Zhao X, Liu Y. The expression landscape of FOXP3 and its prognostic value in breast cancer. *Ann Transl Med* 2022;10(14):801. doi: 10.21037/atm-22-3080